researchvision.us

Symmetria : Journal of Advanced Physics and Mathematical Review
Vol.3 | No. 1 | 2026 pp. 16–25 | ISSN 3066-3636

Experimental Study of Aluminum-Doped Nickel Oxide Thin Films Fabricated Using Pulsed Laser Deposition

Shaimaa Jawad Khudair
College of Science, Tikrit University

Submitted: 8-Feb, 2026
Accepted: 8-Mar, 2026
Published: 12-Mar, 2026

Vol. 3, No. 1, 2026.
10.62762/SJAPMR.2024.000000

***Corresponding author:**
Shaimaa Jawad Khudair [1]

Copyright © 2026 by author(s) and Scientific Research Publishing Inc. This work is licensed under the Creative Commons Attribution International License (CC BY 4.0).

http://creativecommons.org/licenses/by/4.0/

Open Access

Abstract

Thin films of pure nickel oxide (NiO) and Aluminum-doped nickel oxide (NiO-Al, 2%) were prepared and studied using pulsed laser deposition on glass substrates. X-ray diffraction (XRD) analysis revealed that Aluminum doping induces a slight increase in the average crystallite size from approximately 37 nm for the pure samples to about 42.6 nm for the doped films, while maintaining high homogeneity and a smooth surface with vertical roughness not exceeding 31 nm. Field-emission scanning electron microscopy (FE-SEM) results showed that the average grain size of the pure NiO film was 37.82 nm, whereas the doped NiO-Al (2%) film exhibited a larger grain size of 47.65 nm.

Optical characterization indicated an enhancement in absorbance, with absorption coefficients for both pure and doped films reaching values of $\alpha \geq 10^4$ cm $^{-1}$. This confirmed that the electronic transitions in the films were of the allowed direct type. The optical band gap of the pure NiO film was determined to be 3.92 eV, while that of the doped NiO-Al (2%) film decreased to 3.60 eV. The film thickness was measured to be 158 nm. This reduction in band gap is attributed to the introduction of intermediate energy levels within the band gap by Aluminum dopants.

These findings demonstrate that NiO-Al (2%) thin films combine a homogeneous nanostructure, high-quality smooth surfaces, and enhanced, tunable optical response. Consequently, they are promising candidates for advanced applications such as photodetectors, gas sensors, solar cells, and optoelectronic devices with adjustable performance.

Keywords: thin film, pulsed laser deposition, nickel oxide, aluminum

Introduction

Thin films of pure nickel oxide (NiO) and Aluminum-doped nickel oxide (NiO-Al, 2%) were prepared and studied using pulsed laser deposition on glass substrates. X-ray diffraction (XRD) analysis revealed that Aluminum doping induces a slight increase in the average crystallite size from approximately 37 nm for the pure samples to about 42.6 nm for the

doped films, while maintaining high homogeneity and a smooth surface with vertical roughness not exceeding 31 nm. Field-emission scanning electron microscopy (FE-SEM) results showed that the average grain size of the pure NiO film was 37.82 nm, whereas the doped NiO-Al (2%) film exhibited a larger grain size of 47.65 nm.

Optical characterization indicated an enhancement in absorbance, with absorption coefficients for both pure and doped films reaching values of $\alpha \geq 10^4$ cm $^{-1.}$ This confirmed that the electronic transitions in the films were of the allowed direct type. The optical band gap of the pure NiO film was determined to be 3.92 eV, while that of the doped NiO-Al (2%) film decreased to 3.60 eV. The film thickness was measured to be 158 nm. This reduction in band gap is attributed to the introduction of intermediate energy levels within the band gap by Aluminum dopants.

These findings demonstrate that NiO-Al (2%) thin films combine a homogeneous nanostructure, high-quality smooth surfaces, and enhanced, tunable optical response. Consequently, they are promising candidates for advanced applications such as photodetectors, gas sensors, solar cells, and optoelectronic devices with adjustable performance.

1. Interaction of the laser beam with the target material: where the high energy absorption excites the surface of the target.
2. Dynamic Extraction and Extraction of Atoms: Atoms and molecules are uprooted from the surface of the target by the energy gained.
3. Transport and deposition of atoms on the substrate: The uprooted particles are spread within the vacuum chamber to be deposited on the surface of the substrate.
4. Thin film nucleation and crystal growth: The deposited atoms begin to clump and crystallize to form a homogeneous thin film on the surface of the substrate[15].

The practical part

(2-1). Preparation (Maxing out)

99.9% pure nickel and Aluminum powders were used. Use Aluminum as an additive in the ratio of total weight to nickel, which is the base material in the ratio of . After adding the Aluminum to the nickel, the ingredients were mixed in an agate mill for 30 minutes. Then it was placed in a steel mold and pressed for 5 minutes when pressed, after which it was dried in the oven.

(2-2). Method and Deposition

High-purity nickel and Aluminum powder (99.95%) was used. The glass substrates were cleaned using deionized water (DI), methanol, acetone, and isopropyl alcohol. Substrates were then placed on the sample holder inside the evaporation chamber, and nickel powder mixed with Aluminum was deposited at a weight ratio (2 wt%). The powder was heated in a

tungsten boat under approximately pressure. After the deposition process, the thin films were first taken out of the machine, and then placed in a thermal oxidation furnace at a temperature of (400 °C) for two hours, in order to obtain pure NiO films inlaid with Aluminum (Al-doped NiO).).

An Nd: YAG laser beam with a wavelength of 1064 nm, a frequency of 6 Hz, a number of 300 pulses, and a laser energy of 400 mJ, at an angle of 45°, was used inside the deposition chamber under vacuum pressure of Torr. The glass substrates were placed on a stand against the surface of the target. The thin films were then subjected to a thermal annealing process at 400°C for one hour.

To characterize the prepared thin films, X-ray diffraction (XRD), Field Emission Scanning Electron Microscopy (FE-SEM), and Atomic Force Microscopy (AFM) were used and the absorption spectra of the thin films was measured using a visible ultraviolet-vis spectrometer (UV-Vis) within the 300–1100 nm wavelength range.

Results and discussion

1- Synthetic properties

(1-1) Diffraction of X-rays :

The results of the XRD X-ray diffraction showed that the 2% Aluminum graft did not alter the basic crystal phase of NiO, suggesting the formation of a solid solution. Subtle changes in the positions of the peaks (if any) reflect a change in the lattice constant due to the difference in the ionic radius. Any expansion of the peaks. The absence of additional peaks negates the existence of separate phases in large quantities. The crystal size using the NiO angle data shows the peaks at angles ($2\theta\sim$ 37, 43 , 36) The corresponding levels (220), (200) and (111) respectively correspond to the standard nickel oxide card with serial number JCPDS No. 47-1049. The sharp and narrow peaks indicate a high degree of crystallization of the material, the result shows that the width of the mid-peak has increased after FWHM. The grain volume rate was calculated using the Sharar equation of equation (1) and it was found that the measured granular volume values of the pure thin film fall within the range (16.225-109.016) and the granular size of the marred thin film falls within the range (13.62-55.05).

NiO-Al (2%) The Aluminum-grafted sample retains approximately the same locations as the main peaks and this is consistent with studies [16,17]. As illustrated in Figures(1, 2, and 3)

(1-2) Scanning electron microscopy results:

By studying the surface morphology (FESEM) of the prepared (158 , the pure NiO sample has a homogeneous nanogranular structure with an average granular size of about 37 nm, with a narrow size distribution and a uniform spherical shape. These morphological properties make the material a promising candidate for applications that depend on surface phenomena and nanosize. [17].

The NiO-Al (2%) sample exhibits a nanogranular structure with an average grain size of about 42.6 nm, which is slightly larger than the pure sample, suggesting the effect of

Aluminum grafting on growth kinetics. The morphology is homogeneous and porous, making the material good for applications based on surface interactions and optical properties.

This image shows a sample with a nano grainy structure but a much larger grain size (~150 nm) than seen in previous samples, with high porosity and a less homogeneous volumetric distribution. This suggests that the sample was prepared under different conditions (possibly higher annealing temperature or different grafting ratios).

Using the cross-section technique in the scanning electron microscopy, the thickness of the thin film was measured and it was found that the contours of the thin film were regular and moderately deposited, and it was found that the thickness of the thin film was equal to (158)nm. As illustrated in Figures(4, 5, and 6)

$D_{ave}=0.9\lambda\beta\cos\theta$ ..... (1)

Where λ =1.54 Å is the (X-ray) wavelength (Kα-line), β (also called FWHM) is the full-width at half-maximum (in radians),θ is Bragg's diffraction angle

(1-3) Atomic Force Microscope Results: (AFM)

Atomic force microscopy technique was used to study the topography and topography of the prepared thin film surfaces, the extent to which the number of pulses and distortion ratios affect the properties of the prepared thin film, and to give statistical values for grain size and surface roughness based on the square root of the root mean square, where the AFM data of the NiO-Al (2%) sample are shown The thin film has a very smooth surface over an area of 24.2 × 24.2 μm, with a total vertical contrast of only about 31 nm. This reflects high homogeneity and excellent smoothness, making the sample suitable for applications that require high-quality surfaces. These results are consistent with SEM images that showed compact nanograins, and also enhance the reliability of previous optical absorption measurements.

The pure NiO sample exhibits an ultra-smooth surface structure with high homogeneity, with a total vertical contrast of about 24.3 nm over an area of 4.56 × 4.56 μm. This confirms the quality of the film and its usability in optical and electronic applications. In comparison, the Aluminum grafted sample exhibits slightly greater roughness (~31 nm over a wider area), reflecting the effect of grafting on granular growth without compromising the overall quality. These results are consistent with SEM images A comprehensive understanding of the effect of grafting on the morphological characteristics of NiO thin films is strengthened, and this is consistent with the research [18]. As shown in Figure (7)

2-Optical Properties:

The absorption coefficient of the prepared thin films was calculated through equation (2), and the results showed that the best absorption was within the visible area of (300-700) nm of the electromagnetic spectrum, i.e. the absorption increased, and the energy gap is larger, which means that the thin film has high permeability and uses reagents and in the manufacture of

solar cells, and the results showed that the absorption coefficient increases with the increase in the photon energy of the prepared thin films and is of the type of direct transmission allowed, and this indicates that the absorption process occurs in the range. Optical and the possibility of electronic transitions between the valence and conduction beams, Aluminum inlaying leads to a reduction in the energy gap and also control the optical properties and the absorption coefficient of the material can be controlled significantly using light excitation. The higher the excitation energy, the higher the absorption intensity, especially at the high energies of the falling photon. This behavior makes the material used in photodetector applications and this is consistent with the study [18]. As illustrated in Figures (8, 9, and 10)

$(R_\lambda(A_D\Delta f)^{1/2}/I_n \ldots\ldots (2).[\ D^*$

Conclusions

Through our findings from this research, it was concluded that pure NiO films have a super homogeneous nano-granular structure with a very smooth surface, making them an excellent basis for studying the grafting effect with the addition of 2% Aluminum, thus increasing the size of the grains slightly and the optical properties improving rapidly, especially under the photoactive effect while maintaining high surface quality, and also Controlling the preparation conditions such as annealing temperature is very important to avoid large granule growth that may impair performance.

References

[1] M. Naito, T. Yokoyama, K. Hosokawa and K. Nogi, “Nanoparticle Technology Handbook”, 3rd ed., Ch. 1, Springer (2018) p. 3.

[2] W. He et al., “Thin bismuth oxide films prepared through the sol–gel method”, Mater. Lett., 61(19) (2007) 4100 4102.

[3] B. Zohra," Elaboration et caractérisation des couches minces GIS déposé par la technique électrodéposition", mémoire de master, université d'El-oued, Algérie (2016).

[4] l. Filipovic, Member, IAENG, S.2A selberherr, Giorgio C. Mutinati, E. Brunet, S. Steinhauer, A. Kock, J. Teva, J. Kraft, J. Siegert, and F. Schrank,"Modeling spray pyrolysis deposition", proceedings of the world congress on engineering, vol II, London (2013)

[5] **Darbalah, A., & Hamza, A. (2016).** *Nanotechnology and its applications in various fields (Agriculture – Food Technology – Water – Environment – Pest Control).* International Books House, Egypt.(2016) .

[6] **Sabri, F. (2016).** *Nanosenso: Development of smart nanotechnology-based sensors connected to the network for illuminating brain chemistry and early cancer detection* (Trans. N. Qattan). One Billion Enlightened(2023) .

[7] Balu, A., V. Nagarethinam, N. Arunku mar, and M. Suganya. “Performance analysis of semiconductor devices.” Journal of Elec tron Devices, vol. 13, 2012, pp. 920–930.

[8] **Azara Hussein, S., & Jalil Abd Al-Sada, G. (2018).** *Effect of copper doping on the structural properties of zinc ferrite thin films.* Karbala University Scientific Journal, 16(1), 66–85.(2016) .

[9] H. Benzarouk," Synthèse d'un oxide transparent conductor (OTC) par pulvérisation chimique (ZnO ‹NiO)", Mémoire de Magister, Université de Badji Mokhtar, Algérie (2008).

[10] A. Venter, J. Botha," Optical and Electrical properties of NiO for possible dielectric applications", S Afr J Sci.107(1/2), Art.268, vol 107, N 6 pages. 102 (2011).

[11] Enrique luis graue wiechers rector," te la tabla de los elementos", hecho e impreso en méxico (1' edicion), coyoacan (méxico) (2019).

[12] Eugene, A. V. R., G. Gamaly, and Barry Luther-Davies, "Ultrafast Laser Ablation and Film Deposition", (2007).

[13] Siraj. K., PhD thesis, Institute of Applied Physics, Johannes Kepler University Linz, Austria, (2007).

[14] Vilanova X. " Development of a Thin Film Gas Sensor for Oxygen Detection at Trace Levels" Ph.D. Thesis , Helsinki University of Technology (2006) .

[15] Hafizuddin. M., H. Jumali, and M. Yahaya " Comparative Studies on Micro structural and Gas Sensing Performance of TiO_2 and TiO_2-PANi Nanocomposite Thin Films" Solid State Science and Technology, 17, (2009) .

[16] R. Vyas et al., “Synthesis and Hydrogen Sensing Properties of CNT-ZnO nanocomposite thin films", Int. J. Mod. Phys. Conf. Ser., 22 (2013) 478-482.

[17] A.S. Abd-Alsada and M.F.A. Ali, “Impact of CNT Concentrations on Structural, Morphological and Optical Properties of ZnO:CNT Nano composite Films”, J. Phys. Conf. Ser., 2114 (2021) 012020.

[18] R.A. Ahmed et al., “Synthesis and Characterization of CdO1-xZnOx for Solar Cell Applications”, Dig. J. Nanomater. Biostruct., 14(1) (2019) 15-22.

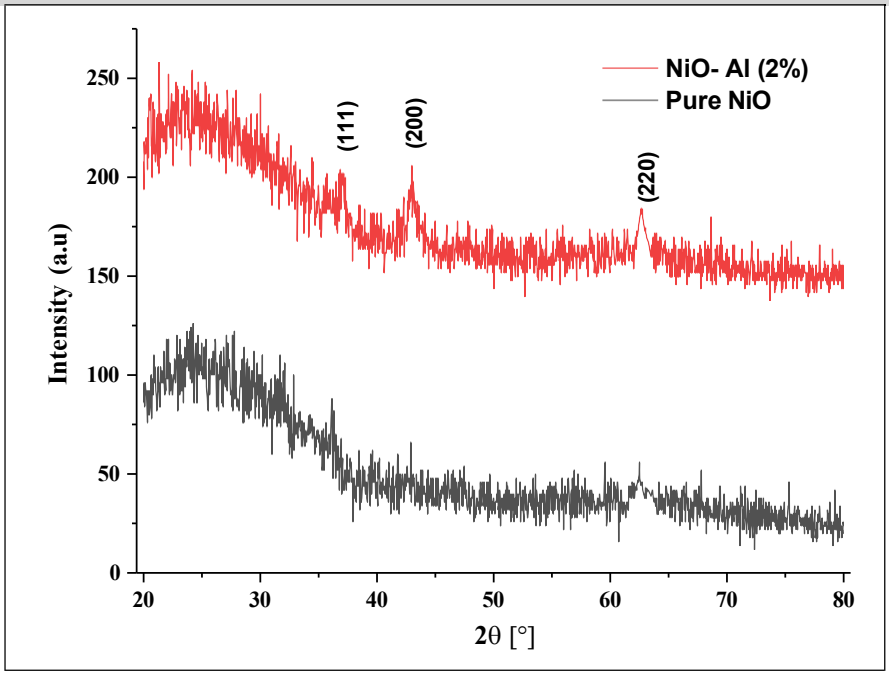


Figure 1: XRD Results of Pure and Impregnated Aluminium Oxide Films on Glass

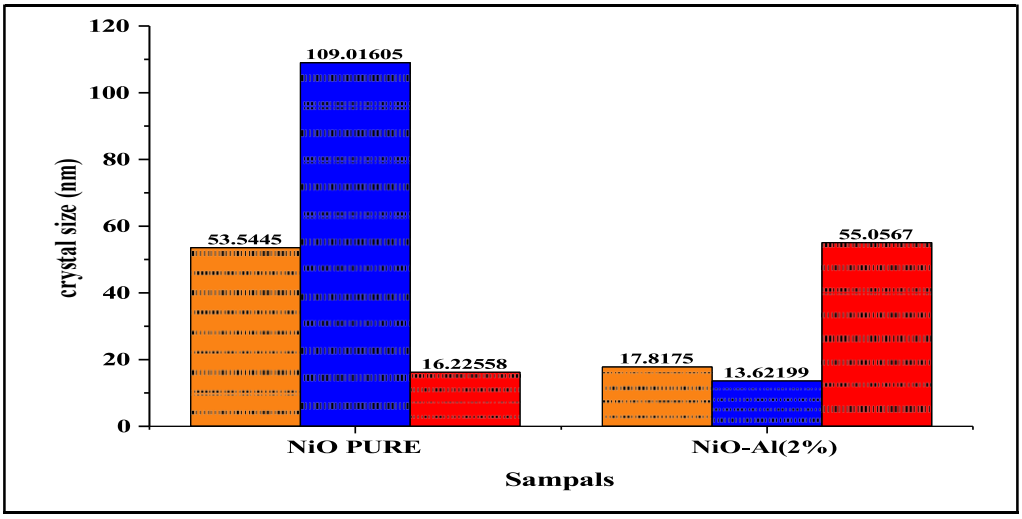


Figure 2 shows the granular size of the pure nickel oxide membrane impregnated with aluminum

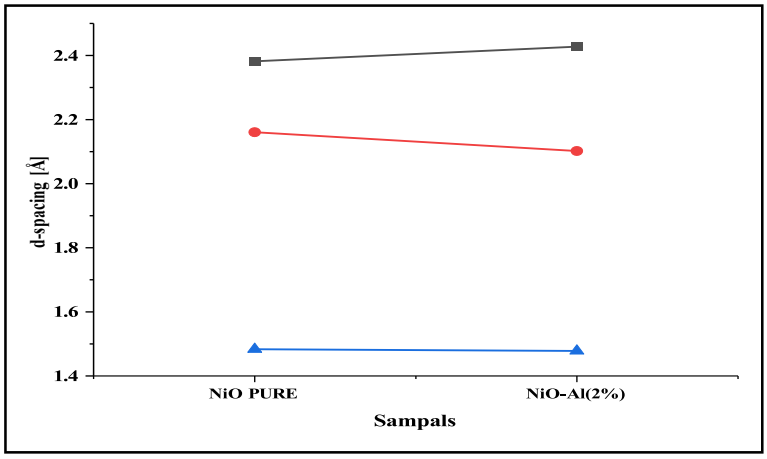


Figure 3 shows the intervals between the pure and aluminium nickel oxide thin film

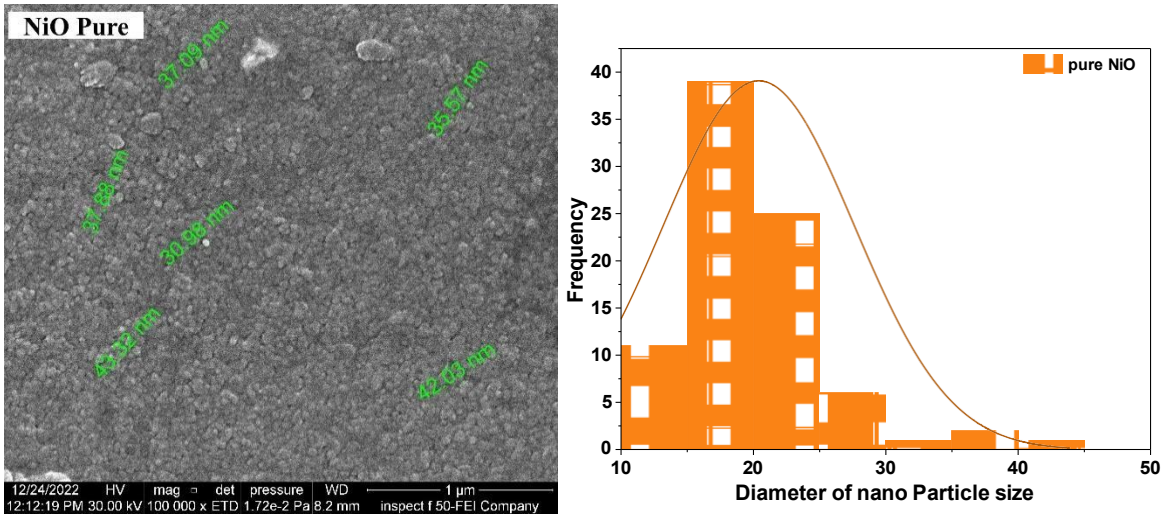


Figure 4 shows the FESEM images of the pure aluminum oxide thin film

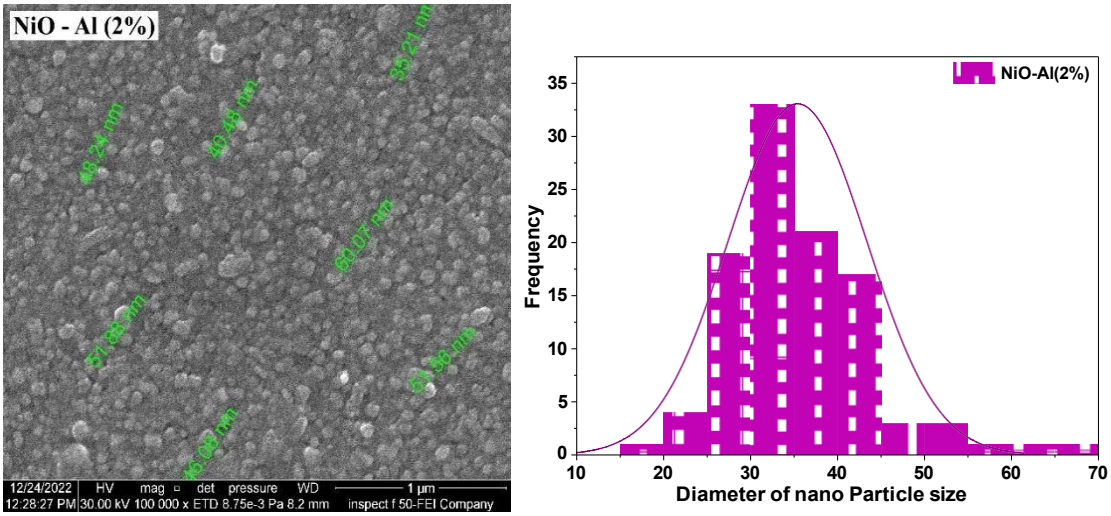


Figure 5 shows FESEM images of nickel oxide membrane impregnated with aluminum

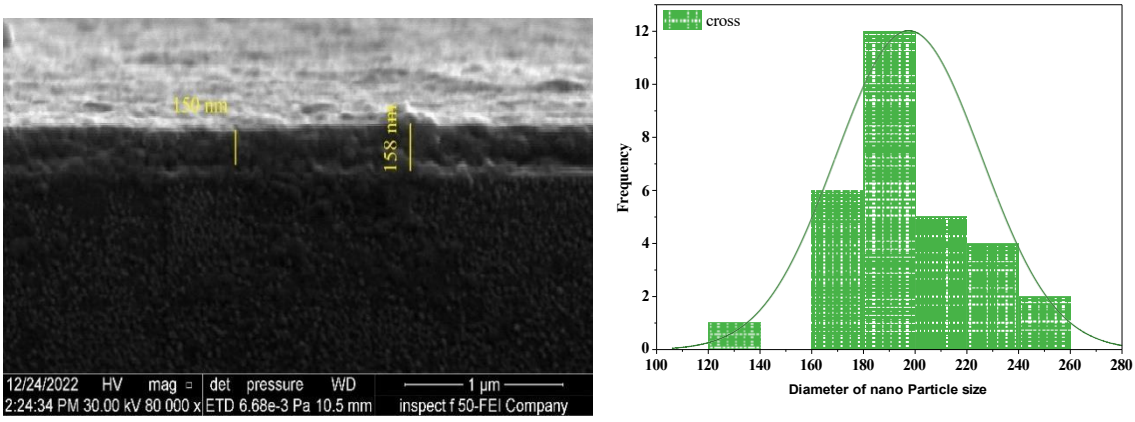


Figure (6) shows the thickness of the thin membrane with the cross-section.

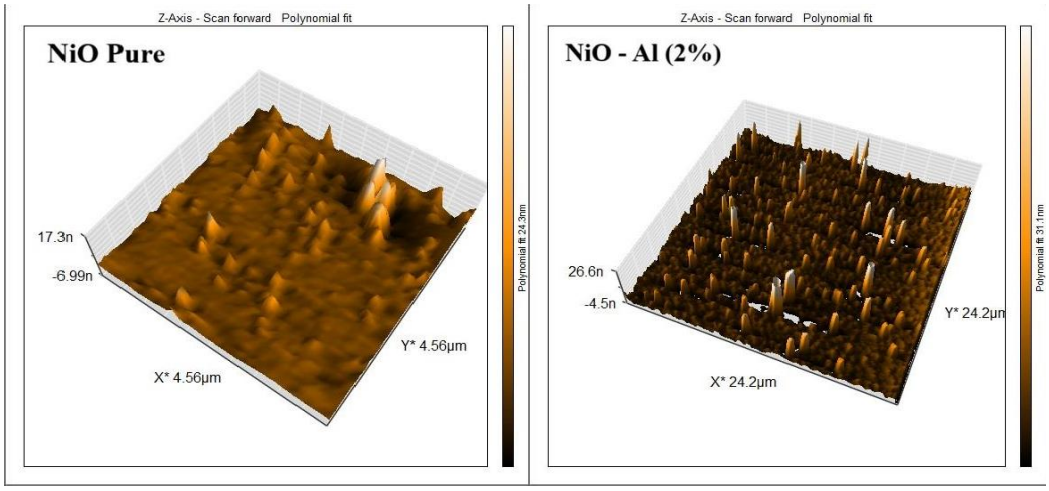


Figure (7) shows the AFM images of the pure nickel oxide membrane and amalgamated

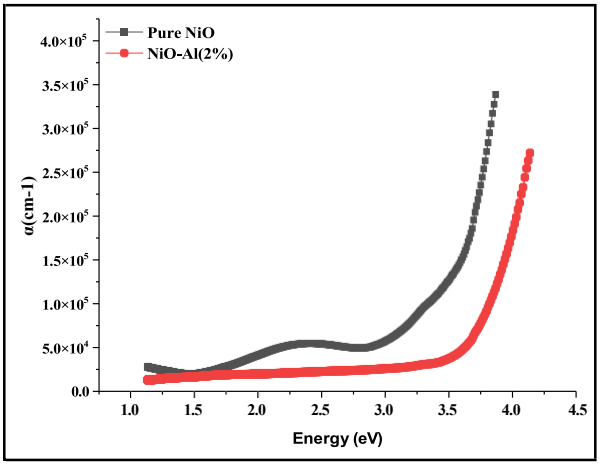


Figure 8) shows the change in the absorption coefficient

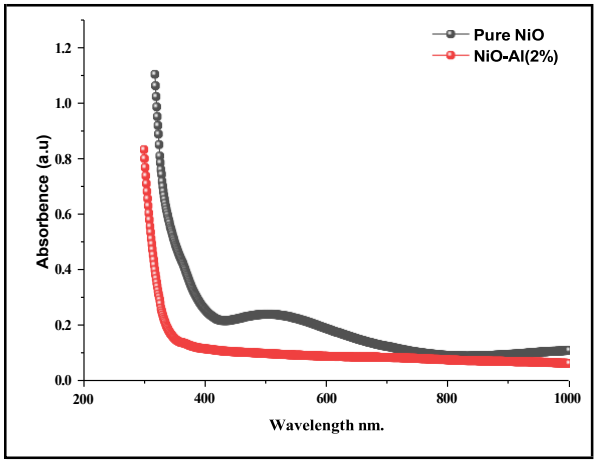


Figure 9 shows the absorption spectrum

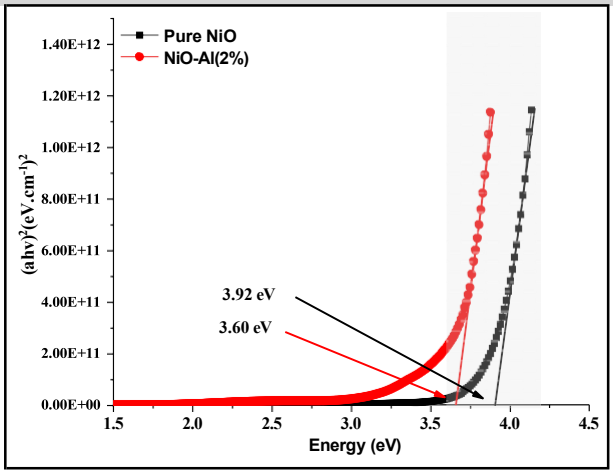


Figure 01 shows the optical energy gap values of pure and amygdalized aluminum oxide membranes